

# Using High Pressure Homogenization (HPH) to Change the Physical Properties of Cashew Apple Juice

Thiago Soares Leite · Pedro E. D. Augusto · Marcelo Cristianini

Received: 11 April 2014 / Accepted: 30 November 2014 / Published online: 7 December 2014  
© Springer Science+Business Media New York 2014

**Abstract** The High Pressure Homogenization (HPH) process is a non-thermal technology that can be used to change the structure of fluid foods. The main transformations are related to the rheology, particle size distribution (PSD) and pulp sedimentation, and the way that each vegetable matrix responds to the HPH process is unique and hard to predict. In the present study, the effect of HPH (up to 150 MPa) was evaluated for cashew apple juice (10 °Brix) in relation to the rheological properties, PSD, optical microscopy and pulp sedimentation during storage. The HPH process decreased the juice consistency coefficient and yield stress (up to 50 % and 30 % of the original values, respectively). The flow behaviour index increased to nearly twice its original value, and the juice thixotropy was slightly reduced. HPH also decreased the mean particle size and changed the PSD. It had no impact on the final sedimentation index, but decreased the velocity of sedimentation. The microstructure could be observed by optical microscopy, which also showed the decrease in particle size. All the parameters were modelled as a function of the homogenization pressure, which could be useful for a better understanding and as an aid in future studies. The results showed that the HPH process could be used to decrease the cashew apple pulp sedimentation velocity, which could lead to the use of a reduced amount of additives.

**Keywords** Cashew apple · Fruit juices · High pressure homogenization · Rheology

## Nomenclature

$\dot{\gamma}$	shear rate [ $s^{-1}$ ]
$\eta$	viscosity [ $Pa \cdot s$ ]
$\eta_a$	apparent viscosity ( $= \sigma / \dot{\gamma}$ ) [ $Pa \cdot s$ ]
$\sigma$	shear stress [ $Pa$ ]
$\sigma_0$	yield stress, Herschel-Bulkley model (Eq. 4) [ $Pa$ ]
$\sigma_e$	equilibrium stress in the Fignon-Shoemaker model (Eq. 3) [ $Pa$ ]
$\sigma_i$	initial stress in the Fignon-Shoemaker model (Eq. 3) [ $Pa$ ]
$\zeta$	zeta potential [ $mV$ ]
$d$	particle diameter [ $\mu m$ ]
$D[4,3]$	mean particle volume-based diameter (Eq. 1) [ $\mu m$ ]
$D[3,2]$	mean particle area-based diameter (Eq. 2) [ $\mu m$ ]
$IS$	sedimentation index (Eq. 5) [–]
$IS_e$	sedimentation index at equilibrium (infinite time) (Eq. 7) [–]
$IS_i$	initial value of sedimentation index (time 0) (Eq. 7) [–]
$k$	consistency coefficient, Herschel-Bulkley model (Eq. 4) [ $Pa \cdot s^n$ ]
$k_B$	Boltzman constant [ $= 1.38 \cdot 10^{-23} N \cdot m \cdot K^{-1}$ ]
$k_{FS}$	kinetic parameter in the Fignon-Shoemaker model (Eq. 3) [ $s^{-1}$ ]
$k_S$	kinetic parameter in the sedimentation index model (Eq. 7) [ $day^{-1}$ ]
$n$	flow behaviour index, Herschel-Bulkley model (Eq. 4) [–]
$Pe$	Peclet number (Eq. 6) [–]
$P_H$	homogenization pressure [ $MPa$ ]
$\bar{r}_{particle}$	mean suspended particle radius [ $m$ ]
$t$	time (Eq. 3) [ $s$ ]

T. S. Leite (✉) · M. Cristianini  
Department of Food Technology (DTA), School of Food Engineering (FEA), University of Campinas (UNICAMP), CEP: 13083-862 Campinas, SP, Brazil  
e-mail: sleite.thiago@gmail.com

P. E. D. Augusto  
Department of Agri-food Industry, Food and Nutrition (LAN), Luiz de Queiroz College of Agriculture (ESALQ), University of São Paulo (USP), Piracicaba, SP, Brazil

t time (Eq. 7) [days]  
 T absolute temperature [K]

## Introduction

The cashew tree is a native Brazilian plant, mainly located in the northeastern and northern regions. Its main product is the cashew nut, the cashew apple (a pseudofruit) mainly being considered as a byproduct of the industry. However, it can be used for juice production. The major problem of cashew apple juice is the sedimentation of its pulp, which requires the use of hydrocolloids to be reduced. Cashew apple juice is a complex product, containing a wide variety of sugars, acids, vitamins and polyphenols, with high contents of carotenoids and ascorbic acid, showing great health benefits on consumption [1–3].

The high pressure homogenization (HPH) process was initially designed to control the microbiological spoilage of liquid foods. Recently, it has been used in order to promote desirable changes in the characteristics of a wide range of products, such as improving the activity and stability of enzymes [4], the properties of polysaccharides [5, 6] and proteins [7] as well as improving the rheological properties of fruit and vegetable juices [8–13].

This technology is a continuous process, in which a fluid is pumped, reaching high pressure levels and then forced through a narrow gap causing a high shear condition. Within the gap, due to the mass and energy conservation laws, the velocity of the fluid drastically increases, leading to a great pressure drop to atmospheric pressure levels in very short time, causing great turbulence and cavitation [14–17]. Consequently, the product components are submitted to high shear and friction, which can change many of its proprieties.

The knowledge of the rheological properties of food products is highly necessary for an understanding of many industrial processes. It is also important for the stability and quality aspects of the final product, and the correlations of these with the sensory qualities and consequently with consumer acceptance [18].

It is not easy to predict the effect of HPH technology on the properties of fruit products. In fact, Lopez-Sanchez et al. [11] showed that each vegetable cell wall had a different behaviour when processed by HPH. While carrot tissue requires higher shears to be disrupted, the tomato cells were broken even at moderate shear values. This suggests that the effect of HPH processing is different for each vegetables product, and highlights the need for a better understanding of this process.

For example, the use of HPH on pineapple pulp reduced its consistency [19], while the opposite behaviour was observed on tomato juice [13]. The rheological properties of a product are heavily dependent on the mean particle size, the particle size distribution (PSD), the shape of the particles and the way they interact with each other and with the serum phase. In

tomato juice, the reduction in particle size contributes to greater interaction, leading to an extensive network which could be observed from the increase in yield stress and consistency. However, in pineapple pulp, smaller particles contributed to a reduced resistance to flow, resulting in a less consistent product.

The effect of HPH on cashew apple juice has still not been studied, although the process could improve some of the aspects of the product, such as reduced pulp sedimentation, which is highly desirable, leading to a reduction in the use of additives to stabilize the pulp. In fact this has been observed for both tomato juice [20] and pineapple pulp [19].

Furthermore, several studies have been carried out with cashew apple fruit, pulp, juice and other products [1–3, 21–24]. However, the rheological properties were only evaluated by Azoubel et al., [22], who did not evaluate the time-dependent properties or the effect of the HPH process. Consequently, the rheology and micro-structure of the cashew apple juice were not studied with much detail.

The objective of this study was to evaluate the effect of HPH on several physical properties of cashew apple juice, such as the PSD, microstructure, pulp sedimentation and rheology.

## Materials and Methods

### Cashew Apple Juice

Pasteurized frozen cashew apple pulp was obtained from a local market, thawed overnight and diluted to 10°Brix with deionized water to obtain a ready-to-drink juice. This concentration was selected as a mean value from various other studies [1–3, 21–24]. The pH of the juice after dilution was 5.0.

### High Pressure Homogenization

The process was carried out at homogenization pressures ( $P_H$ ) of 0 MPa (control), 25, 50, 75, 100 and 150 MPa (gauge values) using a high pressure homogenizer (Panda Plus, GEA Niro Soavi, Italy) in triplicate. The inlet temperature was 25 °C. After the HPH process, the samples were cooled in a water/ice bath then stored at 5 °C until all the analyses had been carried out.

### Particle Size Distribution Analysis

The PSD was evaluated by light scattering (Malvern Mastersizer 2000 with Hydro 2000s, Malvern instruments Ltd, UK), using the spherical model and a refractive index of 1.330. This analysis also provides the mean diameter based on particle volume ( $D[4,3]$ ; Eq. 1) and the mean diameter based on particle surface area ( $D[3,2]$ ; Eq. 2). The  $D[3,2]$  is

more influenced by small particles, while the  $D[4,3]$  is more influenced by the larger ones [9, 10]. All PSD analyses were carried out in triplicate for each sample.

$$D[4, 3] = \frac{\sum_i n_i d_i^4}{\sum_i n_i d_i^3} \quad (1)$$

$$D[3, 2] = \frac{\sum_i n_i d_i^3}{\sum_i n_i d_i^2} \quad (2)$$

### Rheological Analyses

The rheological analyses were carried out at 25 °C using a controlled stress rheometer equipped with a Peltier system (AR2000ex, TA Instruments, USA). Cross hatched plate-plate geometry (40 mm in diameter) was used to prevent slippage of the sample.

A gap-independency procedure was used first, as described by [25]. This consists of varying the distance between the plates until the flow curve does not change, and the gap so obtained was 1300  $\mu\text{m}$ . The maximum shear rate was fixed at 100  $\text{s}^{-1}$ , due to an abnormal behaviour was observed at shear rates above this value that compromised the reproducibility, as described by Fasolin and Cunha [26] and Moelants et al. [27]. The rheological evaluation requires laminar flow, and at higher shear rates, the flow reached the turbulent state, which explains the abnormal behaviour.

The samples were first placed in the rheometer and maintained at rest for 10 min before shearing. After resting, the samples were sheared at a constant shear rate (100  $\text{s}^{-1}$ ) for 300 s, while the shear stress was measured. This fixed shear period was used to ensure that no structural change would happen due shearing after this period, which could compromise the steady-state evaluations, in same time this results could be used to study the time-dependent rheological behaviour of Cashew Apple Juice. The shear stress decay (thixotropy) due to shear time was verified using the Figoni and Shoemaker model (Eq. 3) [28].

After the time-dependent shear period, a linear decreasing stepwise protocol (100  $\text{s}^{-1}$  to 0.1  $\text{s}^{-1}$ ) was used to guarantee steady-state shear conditions for the flow behaviour evaluation. The product flow behaviour was modelled using the Herschel-Bulkley model (Eq. 4), which comprised the Newton, Bingham and Ostwald-de-Waele (power law) models.

$$\sigma = \sigma_e + (\sigma_i - \sigma_e) \cdot \exp(-k_{FS} \cdot t) \quad (3)$$

$$\sigma = \sigma_0 + k\dot{\gamma}^n \quad (4)$$

The parameters for each model (Eqs. 3 and 4) were obtained by nonlinear regression using the software CurveExpert Professional (v.1.6.3, <http://www.curveexpert.net/>, USA) with a significant probability level of 95 %. The parameters for each model (Eqs. 3 and 4) were then expressed using the same procedure as a function of  $P_H$ .

All the rheological analyses were carried out in triplicate for each sample.

### Microstructure

The microstructure was observed using an optical microscope (Carl Zeiss Jenaval, Carl Zeiss Microimaging GmbH, Germany) with a 12.5x lens, digital camera and software (EDN2 Light Microscopy Image Processing System). 30  $\mu\text{L}$  of sample was carefully placed on a glass slide and the droplet covered with a coverslip, which was carefully rotated in 45° in order to guarantee the same orientation for the samples, as described by Bayod and Tornberg [8] and Mert [29].

### $\zeta$ -Potential

The particle charge of the cashew apple juice ( $\zeta$ -potential) was verified using a micro-electrophoresis instrument (Zetasizer Nano-Z model, Malvern Instruments, Malvern, Worcestershire, U. K.). The  $\zeta$ -potential is the measure of electrophoretic mobility of the particles in an oscillating electric field, determined using laser Doppler velocimetry. The analysis was carried out in triplicate and the sample was filtered (11  $\mu\text{m}$ ) before evaluation.

### Pulp Sedimentation

After HPH processing, the triplicate samples were transferred to graduated cylinders and stored under a controlled temperature of 25 °C (BOD TE391, Tecnal, Brazil) for 60 days. Potassium sorbate (0.8 % m/m) was added to prevent microbial growth during storage time. The sedimentation index (IS) was evaluated using Eq. 5 as described by Silva et al. [19] and Kubo et al. [20].

$$IS = \text{sedimentation volume} / \text{total sample volume} \quad (5)$$

### Statistical Evaluation

When relevant, the effect of  $P_H$  was evaluated using the analysis of variance (ANOVA) and the Tukey test at a 95 % confidence level. The Statistica 7.0 (StatSoft, Inc., USA) software was used for this purpose.

## Results and Discussion

### Particle Size Distribution

Figure 1 shows the effect of HPH on the PSD of cashew apple juice. As expected, the mean particle size decreased with increase in  $P_H$ , similar to that observed by other authors with different vegetable matrices [12, 13, 19, 27].

The  $D[4,3]$  value was four times higher than the  $D[3,2]$  value for all the samples, confirming there were a higher amount of bigger particles than smaller ones, as could be seen in Figs. 1 and 2. Both  $D[4,3]$  and  $D[3,2]$  decreased with increase in  $P_H$ , reaching reductions equivalent to ~35 % (25 MPa) and ~18 % (150 MPa) of the initial diameter (control).

Figure 1 also shows that the shape of the PSD become narrower with increasing  $P_H$ . The control sample showed a range of PSD between ~20 and ~1000  $\mu\text{m}$ , while at 150 MPa it showed a range between ~0.5 and ~150  $\mu\text{m}$ . All the processed samples showed an increase in the amount of small particles (1 to 5  $\mu\text{m}$ ), demonstrating that particle disruption took place up to a specific value, related to the equipment dimensions. Thus asymptotic behaviour could be observed in relation to the effect of HPH, i.e., the higher the pressure the lesser its relative impacts on the PSD. Equivalent results were shown by Augusto et al., [13], Silva et al., [19] and Sentandreu et al., [12] for tomato juice, pineapple pulp and orange juice, respectively.

### Microstructure

Figure 3 shows the microstructure of the cashew apple juice as seen by optical microscopy. It can be seen that

the control sample showed almost intact cells and forming clusters. As the  $P_H$  increased, so cell fragmentation could be seen, similar to that observed by Moelants et al., [27] in carrot suspensions and by Kubo et al., [20] in tomato juice, both processed by HPH.

As the  $P_H$  increased, the cell fragments become smaller, and more cell content is released into the dispersed phase. Moreover, the increase in the number of small particles was related to the formation of more fragments of membrane and cell walls. This is in agreement with the results of the PSD analysis, which showed a reduction in particle size, and the increasing of the number of small particles.

As discussed by Moelants et al., [27], not only the size, but also the type and shape of these particles can change the rheological characteristics of a fluid. At higher pressures, particles are smaller leading to a minor resistance to flow, if compared to the clusters of cells present in the control sample. Furthermore, the structure of the processed sample showed a smoother surface, suggesting less resistance to flow.

### $\zeta$ -Potential

The  $\zeta$ -potential determined for cashew apple juice was about -5 mV for all treatments, with no statistical difference between them ( $p > 0.05$ ). Thus the  $\zeta$ -potential was not changed by the HPH process (data not shown).

The cashew juice showed a low  $\zeta$ -potential value (in module) as compared to other products, such as cloudy apple juice (-10.7 mV for the native pH [30]) and orange juice (-20 mV at pH 3.5, and -30 mV at pH 5.0 [31]) The electrostatic charge on the particles is measured by the

**Fig. 1** Effect of HPH on the particle size distribution (PSD) of cashew apple juice

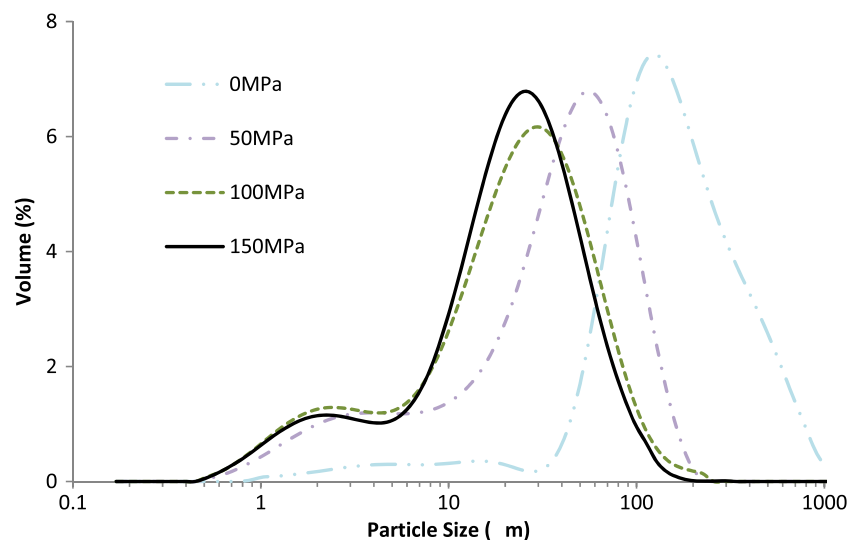
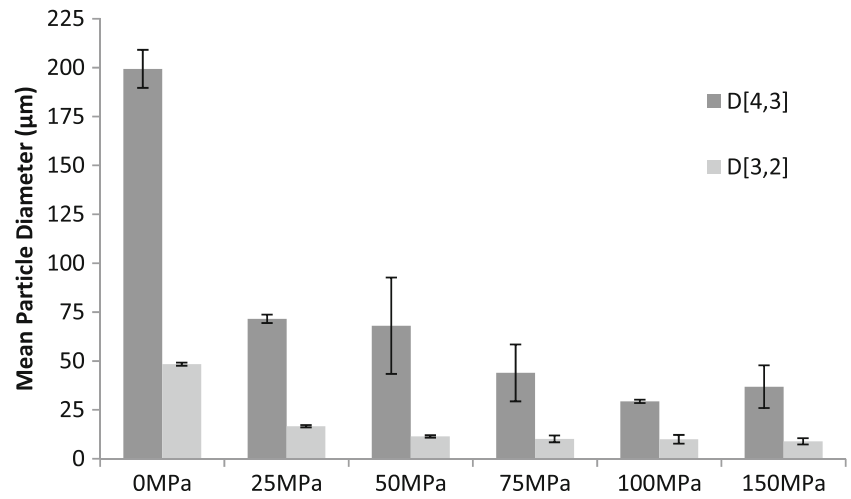


**Fig. 2** Effect of HPH on the mean particle diameters (D[4,3] and D[3,2]) of cashew apple juice (vertical bars are standard deviation)



ζ-potential value [31], so these particles did not show much interaction between them or with the water in the

serum. Therefore little particle aggregation was expected, directly reflecting the product rheology.

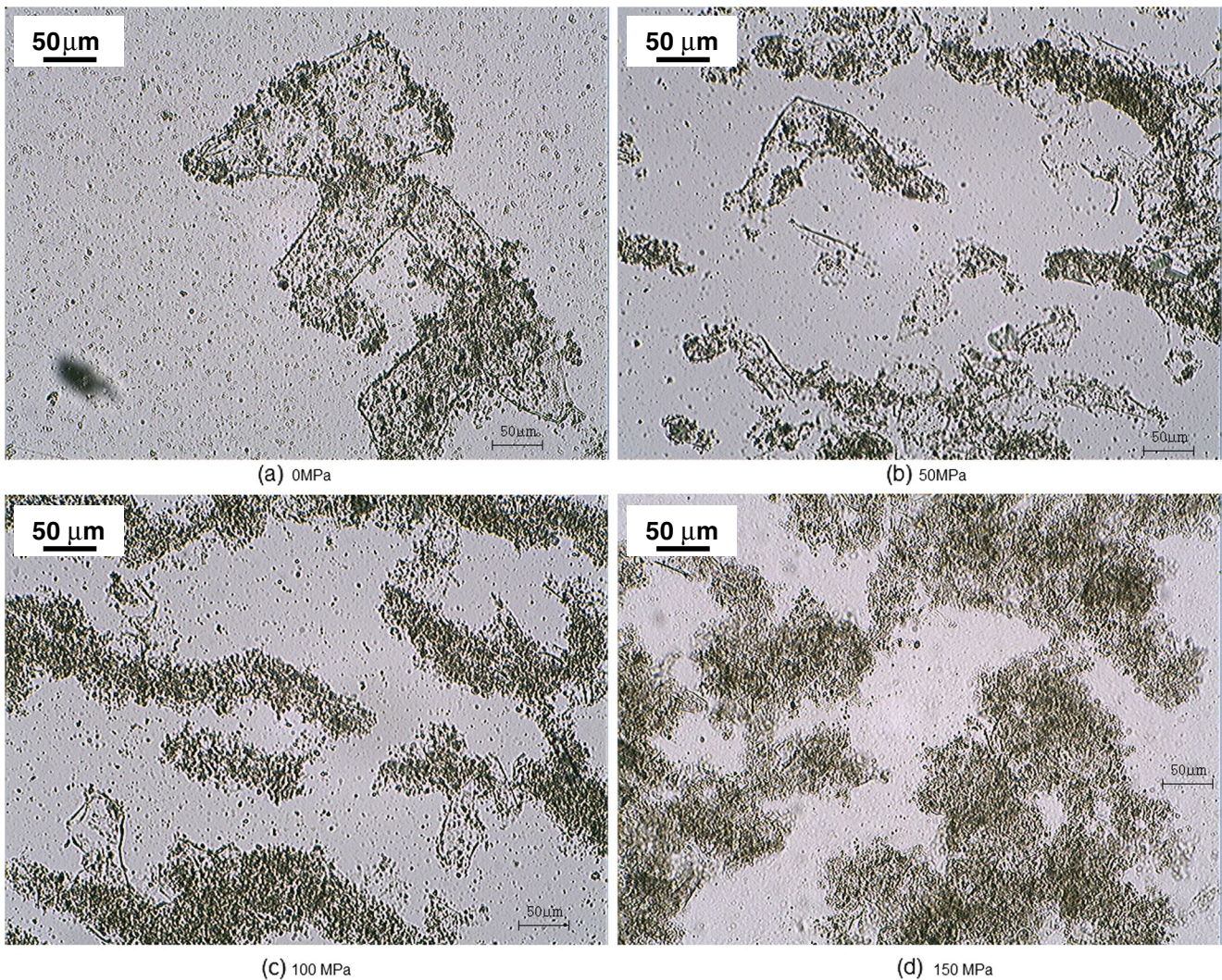
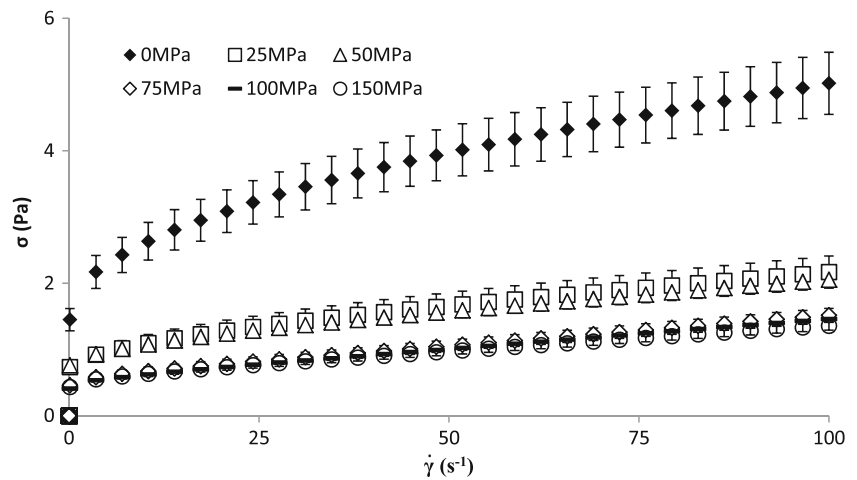


**Fig. 3** Optical microscopy of cashew apple juice at different homogenization pressures. The bar is a reference and has a length of 50 µm

**Fig. 4** Flow curve of cashew apple juice processed at various homogenization pressures at 25 °C (the dots are the mean values, and the vertical bars are the standard deviation)



## Rheological Behaviour

### Effect of HPH on Steady State Flow Behaviour

Figure 4 shows the effect of HPH on cashew juice flow behaviour. The juice showed shear thinning behaviour with yield stress and the flow behaviour could be described by the Herschel-Bulkley model. The Herschel-Bulkley parameters of the non processed juice were compared with other vegetable products in Table 1.

It is clear that HPH reduced the juice consistency, as can be seen in Fig. 4. The HPH processed samples showed lower shear stresses ( $\sigma$ ) for a given shear rate ( $\dot{\gamma}$ ), when compared with the non homogenized samples. Moreover, an asymptotic behaviour could be observed, since the main changes took place at “lower”  $P_H$ , the changes being smaller at “higher”  $P_H$ . The changes are due to the reduction in suspended particles, and are in accordance with the values observed for PSD (Figs. 1 and 2).

Figures 5 and 6 show the effect of HPH on the Herschel-Bulkley model parameters. Both the consistency coefficient ( $k$ ) and yield stress ( $\sigma_0$ ) decreased in an asymptotic way with increase in  $P_H$ , while the flow behaviour

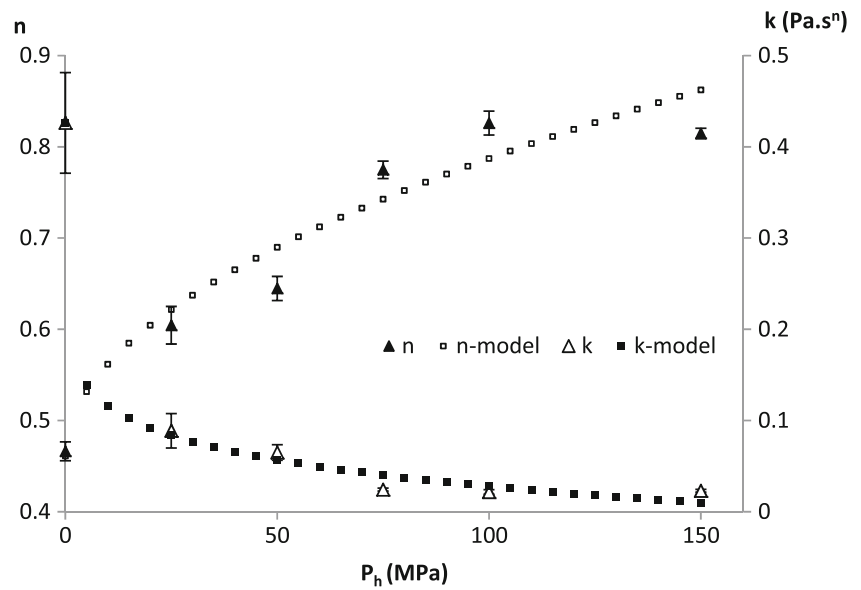
index ( $n$ ) showed the opposite behaviour. The parameter  $k$  decreased from 0.426 to 0.023 Pa.s<sup>n</sup>, while  $n$  increased from 0.466 to 0.815 in the same range of  $P_H$  (from control sample to 150 MPa).

This data is similar to that of Silva et al., [19] for pineapple pulp, where the value for  $k$  decreased from 3.48 to 0.24 Pa.s<sup>n</sup>, and  $n$  increased from 0.29 to 0.55 with increase in  $P_H$  from control sample to 70 MPa. It is important to highlight that the pineapple pulp evaluated by Silva et al., [19] showed shear-thinning behaviour, and thus showed no yield stress, while the cashew apple juice showed pseudoplastic behaviour with yield stress, i.e., Herschel-Bulkley behaviour. Although a direct comparison cannot be carried out due to this difference in the rheological behaviour, a general trend can be considered. The behaviour of the cashew apple juice was also compared to that of tomato juice (a Herschel-Bulkley fluid) as described by Augusto et al. [13]. The tomato juice also showed the same decreasing behaviour of  $k$  from 11.0 to 5.0 Pa.s<sup>n</sup>, and increasing behaviour of  $n$  from 0.4 to 0.9, with increase in  $P_H$ . However, HPH increased the consistency of the tomato juice due to the increase in its  $\sigma_0$ , whereas cashew apple juice showed the opposite trend.

**Table 1** Common values of Herschel-Bulkley parameters of vegetables products

Product	T (°C)	$\sigma_0$ (Pa)	$k$ (Pa.s <sup>n</sup> )	$n$ (-)	Reference
Cashew apple juice (0 MPa)	25	1.336	0.42	0.46	Present Work
Tomato juice	25	5.38	0.92	0.44	[13]
Peach juice (10 % fiber)	20	3.26	13.1	0.46	[42]
Concentrated tamarind juice (71 ° Brix)	30	1.46	4.32	0.59	[43]
Concentrated orange juice	25	2.2	3.13	0.64	[44]
Açaí pulp	25	4.35	0.17	0.78	[25]
Jaboticaba pulp	25	1.55	0.48	0.6	[45]
S. purpurea L. pulp	20	13.26	15.22	0.3	[46]
Batia Pulp	20	32.54	0.15	0.86	[47]

**Fig. 5** Modelling the consistency index ( $k$  -  $\Delta$ ) and the flow behaviour index ( $n$  -  $\blacktriangle$ ) of Herschel-Bulkley model as a function of the homogenization pressure. (Triangles are the mean value of experimental data, vertical bars are the standard deviation, and dotted lines are the models)



The increase in  $n$  and decrease in  $k$  can be explained by the reduction in particle size due to disruption of the juice suspended solids. After the HPH process, there were a larger number of smaller particles than in the original juice, as can be seen in Fig. 1, changing the proportion of small to large particles. This resulted in a greater lubricant effect of the smaller particles on the larger ones, with a consequent reduction in the resistance to flow [32], which was reflected in the reduction in  $k$ . In fact, the amount of particles between 1 and 10  $\mu\text{m}$  increased greatly, as described before (Fig. 1). The changes in the particle surface and geometry, which changed from a rough morphology with many edges to a smooth morphology (Fig. 3), also suggested a reduction in the resistance to flow, and consequently, to a reduction in product consistency.

The Peclet Number ( $Pe$ ; Eq. 6) is a dimensionless number related to the ratio between particle transport due to shearing (non-Brownian systems) and diffusion (Brownian systems) [33]. As the particle size is reduced ( $\bar{r}_{particle}$ ), the  $Pe$  decreases, and the system approximates a Brownian domain. Furthermore, fruit juices and pulps are constituted of two parts: the serum and the dispersed phase. The serum is mainly the water plus all the other soluble components, such as acids, sugars and polysaccharides, while the dispersed phase is composed of all the insoluble matter, such as fibres, whole, disrupted or fragmented cells, and chains or clusters of insoluble polymers suspended in the serum. Consequently, since the HPH reduced both the apparent diameter (since it is not spherical) of the suspended particles (Figs. 1 and 2) and the

**Fig. 6** Modelling of the yield stress ( $\sigma_0$ ) of the Herschel-Bulkley model as a function of the homogenization pressure ( $\blacklozenge$  are the mean values of the experimental data, vertical bars are the standard deviation, and the dotted line is the model)

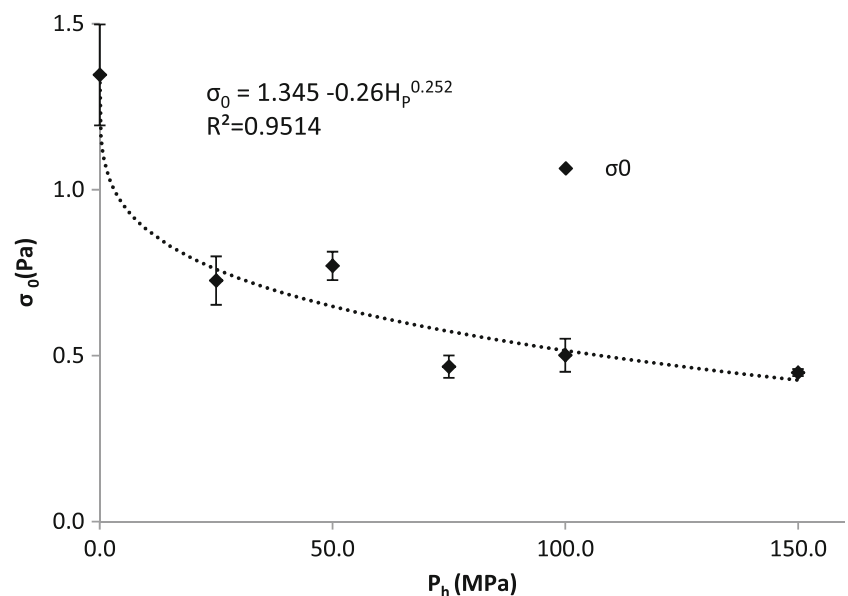


**Table 2** Parameters of the Herschel-Bulkley model as a function of the homogenization pressure (mean±standard deviation; same letters in columns are not significant different)

$P_H$ (MPa)	$\sigma_0$ (Pa)	$k$ (Pa.s <sup>n</sup> )	$n$ (–)
0	1.346±0.152 a	0.426±0.055 a	0.466±0.010 a
25	0.726±0.073 b	0.089±0.019 b	0.604±0.021 b
50	0.770±0.043 b	0.065±0.009 bc	0.645±0.013 c
75	0.467±0.034 c	0.024±0.002 c	0.775±0.010 d
100	0.501±0.050 c	0.022±0.003 c	0.826±0.013 e
150	0.449±0.010 c	0.023±0.002 c	0.815±0.006 e

viscosity of the juice serum [35], it also reduced the Pe of the juice.

$$Pe = \frac{\eta_{\text{continuous phase}} \bar{r}_{\text{particle}}^3 \dot{\gamma}}{k_B \cdot T} \quad (6)$$

At small Pe values (small shear rates or small particles), Brownian motion dominates, while at higher Pe values (higher shear rates or larger particles), structural distortions due to shear flow are more pronounced, and Brownian motion cannot restore the structure of the suspension to its equilibrium state. Therefore shear thinning behaviour occurs [33] and the product rheology is dictated by the hydrodynamic forces. In fact, the homogenized samples showed a flow behaviour closer to Newtonian behaviour, moving away from shear-thinning behaviour, as  $n$  got closer to 1.0 (Fig. 5 and Table 2). Thus, the alignment effect due to flow tended to be less expressive as the suspended particles became smaller and more uniform. This explains the increase in the cashew apple juice  $n$  due to HPH processing.

$\sigma_0$  of cashew apple juice decreased due to the HPH process from an initial value of 1.34±0.152 Pa to 0.44±0.010 Pa (150 MPa). This was similar to that observed with carrot suspensions [27] or applesauce [36]. However, this result

contrasted with that observed by Augusto et al. [13] with tomato juice, where the value for  $\sigma_0$  increased from 5 Pa (control sample) to 12 Pa at 150 MPa due to the HPH process.

The explanation for the reduction in cashew juice  $\sigma_0$  is related to the particle composition, structure, geometry and disruption, as well as to the interparticle (as the Van der Waals and electrostatic) and hydrodynamic forces.

The HPH processed cashew juice showed an increase in the amount of small particles (~1 to 10  $\mu\text{m}$ ), but still contained particles larger than 10  $\mu\text{m}$ . Genovese et al. [34] evaluated the forces involved in the rheology of fluids containing dispersed particles. According to this evaluation, the flow of the larger particles is governed by hydrodynamic forces (since it results in higher Pe values). However, the forces involved in the flow of small particles are a function of the shear rate, according to the Pe. At high shear rates, these particles are governed by the same hydrodynamic forces, while at low shear rates, the interparticle-Brownian forces govern the apparent viscosity ( $\eta_a$ ), network formation and  $\sigma_0$  of the product. Even with negligible interparticle interaction, other non-hydrodynamic properties can change the flow behaviour, such as polarity of the liquid and particle deformability, which will also lead to  $\sigma_0$  [37]. Therefore, when at rest, even particles with small interactions can show  $\sigma_0$  behaviour.

A decrease in particle size generally increases the volume fraction of the particles, and consequently, the inter-particle forces and  $\sigma_0$ , mainly due to the increase in specific particle surface. This can lead to a greater adsorbed water layer, as well as other particle-particle and particle-serum interactions [11, 38, 39]. This explains the increase in the value for  $\sigma_0$  of tomato juice due to HPH processing [13]. However, in the present study,  $\sigma_0$  decreased with the reduction in particle size, which can be attributed to the properties of the cashew apple pulp.

For a given volume fraction and PSD, a hard sphere system always displays a minimum viscosity, and shear yield stress will not occur until the maximum packing fraction is reached.

**Fig. 7** Shear stress with time, (thixogram) of cashew apple juice processed by HPH (dots are the mean value, vertical bars are the standard deviation)

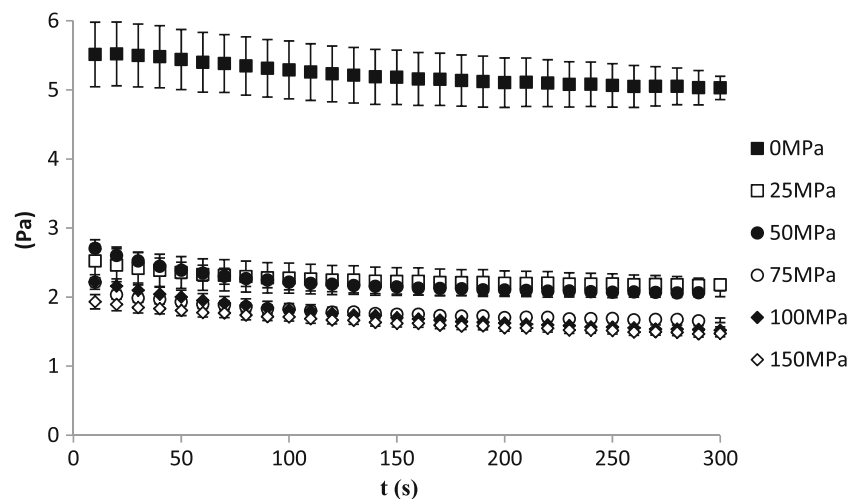




**Table 3** Parameters of the Figoni-Shoemaker model as a function of the homogenization pressure (mean±standard deviation; same letters in columns are not significant different)

$P_H$ (MPa)	$\sigma_i$ (Pa)	$\sigma_e$ (Pa)	$k_{FS}$ ( $s^{-1}$ )
0	5.60±0.53 a	4.88±0.43 a	0.006±0.002 a
25	2.55±0.35 b	2.17±0.24 b	0.014±0.002 b
50	2.79±0.11 b	2.06±0.12 b	0.015±0.001 b
75	1.80±0.12 c	1.33±0.06 c	0.009±0.001 a
100	2.27±0.13 bc	1.45±0.09 c	0.008±0.001 a
150	1.94±0.10 c	1.33±0.01 c	0.005±0.001 a

The introduction of any other kind of interaction, either attraction or repulsion, will result in an increase in suspension viscosity, and, in some cases,  $\sigma_0$  could be observed. An increase in the viscosity and/or  $\sigma_0$  is determined by the magnitude of the overall interactions and the microstructure of the suspension generated by the interactions [40]. Thus the non-hydrodynamic forces can be important in systems with smaller suspended particles, such as HPH juices [13].

The suspended particles in the cashew apple juice were not perfect spheres, which can be observed by the different values of D[4,3] and D[3,2] and by optical microscopy (Fig. 3). In addition, HPH increased the amount of smaller particles in relation to the larger ones, as can be seen in Fig. 1. Thus the smaller particles can fill the spaces between the larger ones, whose lubricant effect reduces the overall resistance to initiate flowing [32].

Therefore HPH reduced the cashew apple Pe number (due to the reduction in both the mean particle size -  $\bar{r}_{particle}$  and the serum viscosity), approximating it to the Brownian domain. Since the  $\sigma_0$  was decreased, it can be inferred that the hydrodynamic (mechanical) forces dictated the product rheology, whereas the non-hydrodynamic forces (such as Van der Waals and electrostatic forces) had a less pronounced effect.

The  $\zeta$ -potential of the particles showed a small electric charge, and consequently there was little electrostatic interparticle interaction. However,  $\sigma_0$  is observed in the product, which can be attributed to other weak forces, such as Van-der-Waals forces, forming a weak network in low shear rates (or small Pe), which is easily broken on higher shear condition.

Those forces were not improved by an increase in the particle surface area.

As shown by Lopes-Sanchez et al. [10], each vegetable matrix reacts in a different way to the HPH process, because different shear stresses can be required to disrupt some cells and tissues due to a variety of factors, such as the chemical composition of the cell walls and crosslinking between the polysaccharides. Once again this highlights the need for a better understand of the effect of HPH on different vegetable products.

*The effect of HPH on Time-Dependent Behaviour*

The cashew apple juice showed low thixotropy, which can be observed from the slow decrease in shear stress with time of shearing (Fig. 7). This was confirmed by the parameters of the Figoni-Shoemaker model (Table 3), showing an initial stress of 5.60 Pa and reaching equilibrium at 4.88 Pa. Thus the difference between the initial and equilibrium shear stresses was small ( $\sigma_i - \sigma_e=0.72$  Pa) as compared with the other products shown in Table 4.

The  $k_{FS}$  (Table 3) parameter is related to the rate of breaking of the structure. The non homogenized sample showed a value of  $0.0064 s^{-1}$  at a constant shear of  $100 s^{-1}$ , which was similar to that of other products, as shown in Table 4.

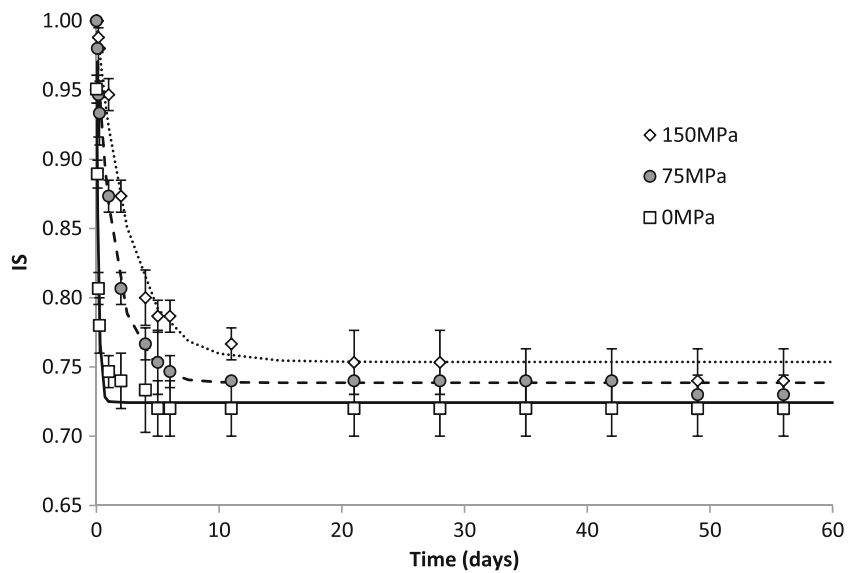
After homogenization, both shear stress parameters decreased ( $\sigma_i, \sigma_e$ ), which showed a less thixotropic tendency (Table 3). Thixotropy is related to the change in structure due to shear and destruction of the internal structure or disaggregation of aggregates during flow [8, 41, 52]. This can be seen from the decreases in apparent viscosity ( $\eta_a$ ) and shear stress with time decreasing, at the same shear rate, over the time [18]. Therefore, the presence of the thixotropic behaviour can be used as a parameter to evaluate the particle tendency of forming aggregates, caused by inter-particles forces. As previously described, these forces are negligible on high shear rates [34], i.e., higher Pe values. Then, when the sample is sheared, these forces cannot maintain the network, and the aggregates collapses.

The HPH process tends to decrease the difference of initial stress and the equilibrium stress ( $\sigma_i - \sigma_e$ ), as well as they absolute values (Table 3), showing that the cashew juice after the process

**Table 4** Common values of Figoni-Shomaker model’s kinetic parameter ( $k_{fs}$ )

Product	T (°C)	$\gamma$ ( $s^{-1}$ )	$\sigma_i - \sigma_e$ (Pa)	$k_{FS}$ ( $s^{-1}$ )	Reference
Cashew apple juice (0 MPa)	25	100	0.72	0.006	Present Work
Gilaboru (43 °Brix)	20	100	5.33	0.0029	[48]
Pineapple jam	–	10–100	–	0.0024–0.0094	[49]
Chickpea flour dispersion	20	100	40	0.0055	[50]
Tomato juice	25	300	0.81	0.0056	[46]
Concentrated orange juice	0	70	120.8	0.693	[51]

**Fig. 8** Sedimentation Index (IS) of cashew apple juice processed by HPH with time (dots are the mean value, vertical bars are the standard deviation, lines are the models with time)



became less thixotropic. Then, it is evident that there is not strong aggregation, which is in agreement to the  $\sigma_0$  results.

It was not possible to notice a tendency caused by HPH on  $k_{FS}$ , ( $p < 0.05$ ). Thus, summed to the product low thixotropy, which can be negligible in industrial processing, the time dependent properties were not modelled as a function of  $P_H$ .

**Pulp Sedimentation**

Pulp sedimentation is a common problem in cashew apple juice. The effect of various  $P_H$  values on the sedimentation index (IS, Eq. 5) of cashew juice with time is shown in Fig. 8 (just some of the processing pressures were plotted, for better visualization). It was modelled using an equation related to the initial value, the equilibrium value and the rate of sedimentation (Eq. 7), as described by Kubo et al. [20].

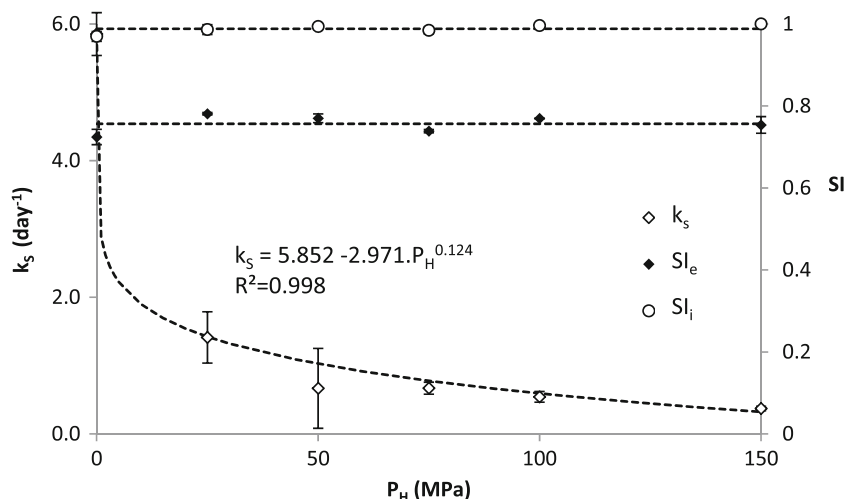
$$IS = IS_e + (IS_i - IS_e) \cdot \exp(-k_S \cdot t) \tag{7}$$

The control juice showed a faster decrease in IS, and took approximately 5 days to reach equilibrium. The 75 MPa sample reached approximately the same IS value in about 1 week, while the higher  $P_H$  sample (150 MPa) reached equilibrium around the 18th day. However, independent of  $P_H$ , all the samples reached approximately the same equilibrium value for IS of around 0.75 (with no difference at 5 % of significance).

A decrease in  $k_S$  was observed for pineapple pulp, but the final value for IS was different for each pressure [19]. With tomato juice, to the contrary, none of the processed samples showed sedimentation, the IS remaining at 1.0 throughout the 60 days of the experiment [20]. This also confirms the work of Lopes-Sanchez et al., [10, 11], who stated that each vegetable matrix reacted in its own way to the HPH process.

Stokes Law states that the particle sedimentation velocity is proportional to the squared diameter of the particle (assuming spherical particles), the difference between the densities of the particles and the dispersed phase, and inversely proportional

**Fig. 9** The effect of HPH on the sedimentation parameters (dots are the mean values of the experimental data, vertical bars are the standard deviation, dotted lines are the curve models)



to the dispersed phase viscosity. It is important to observe that Stokes Law describes a system where only mechanical forces are acting. Therefore, if the particles interact one with the other (due to electrostatic and Van der Waals forces, for example), this Law cannot explain the whole phenomenon.

Figure 1 shows the reduction in particle size. Considering the low impact of the HPH process on serum viscosity [35], it was to be expected that HPH would reduce the cashew apple particle sedimentation rate, and, in fact, this was the behaviour observed (Fig. 8).

It was also indicative that inter-particle forces of the cashew apple were not changed by the HPH process, and remained weak (low  $\zeta$ -Potential). In addition,  $\sigma_0$  decreased resulting in a weaker network, reflected by the fact that the particles did not form aggregates. If such aggregates were observed, this could avoid sedimentation, as observed by Kubo et al. [20], which was not the case in this study. The sedimentation of cashew apple juice pulp was not avoided and only Stokes Law could be used to explain this phenomenon.

Finally, the behaviour of IS with time was modelled using Eq. 7 for each processing pressure used, as shown in Fig. 8. In addition these parameters were modelled as a function of  $P_H$ , as shown in Fig. 9. In fact only the rate of sedimentation ( $k_s$ ) was modelled, since the other two parameters ( $IS_e$  and  $IS_i$ ) were not influenced by the HPH process ( $p < 0.05$ ) and thus the mean value obtained could be used. As expected, the rate of sedimentation showed an asymptotic tendency, as observed with the other results.

## Conclusions

The HPH process disrupts clusters of cashew apple cells and whole cells forming small fragments, as observed by optical microscopy and laser diffraction, causing a reduction in the mean particle diameter and in the PSD. Particle disruption resulted in rheological changes, such as an increase in  $n$ , and decreases in both  $\sigma_0$  and  $k$ , and could be modelled as a function of  $P_H$ . These models can be used for a better understanding of the effects of HPH on cashew apple juice.

The low value of the  $\zeta$ -potential and the reduction in both product thixotropy and  $\sigma_0$  after HPH, showed there were little juice particle interactions, and there was no further particle aggregation. The HPH process did not change the final sedimentation index, but did change the rate of sedimentation ( $k_s$ ), also explained by the reduction in particle size, which could lead to better consumer acceptance.

**Acknowledgments** The authors are grateful to the São Paulo Research Foundation (FAPESP) for funding projects no. 2010/05241-8, 2010/05240-1, 2012/15352-9 and 2012/17381-4.

## References

1. R.B. Assunção, A.Z. Mercadante, *Food Chem.* **81**, 495–502 (2003)
2. R.B. Assunção, A.Z. Mercadante, *J. Food Comp. Ana.* **16**, 647–657 (2003)
3. K.D.P. Silva, F.P. Collares, J.R.D. Finzer, *Food Chem.* **70**, 247–250 (2000)
4. A.A.L. Tribst, P.E.D. Augusto, M. Cristianini, *Int. J. Food Sci. Technol.* **47**, 716–722 (2012)
5. B. Wang, D. Li, L.J. Wang, Y.H. Liu, B. Adhikari, *J. Food Eng.* **113**, 61–68 (2012)
6. T. Wang, X. Sun, Z. Zhou, G. Chen, *Food Res. Int.* **48**, 742–747 (2012)
7. X. Dong, M. Zhao, B. Yang, X. Yang, J. Shi, Y. Jiang, *J. Food Process Eng.* **34**, 2191–2204 (2011)
8. E. Bayod, E. Tomberg, *Food Res. Int.* **44**, 755–764 (2011)
9. H. Bengtsson, E. Tomberg, *J. Texture Stud.* **42**(4), 268–280 (2011)
10. P. Lopez-Sanchez, J. Nijse, H.C.G. Blonk, L. Bialek, S. Schumm, M. Langton, *J. Sci Food Agric.* **91**, 207–217 (2011)
11. P. Lopez-Sanchez, C. Svelander, L. Bialek, S. Schumm, M. Langton, *J. Food Sci.* **76**(1), E130–E140 (2011)
12. E. Sentandreu, M.C. Gurra, N. Betoret, J.L. Navarro, *J. Food Eng.* **105**, 241–245 (2011)
13. P.E.D. Augusto, A. Ibarz, M. Cristianini, *J. Food Eng.* **111**, 570–579 (2012)
14. J. Floury, J. Belletre, J. Legrand, A. Desrumaux, *Chem. Eng. Sci.* **59**, 843–853 (2004)
15. C.R.G. Pinho, M.A. Franchi, P.E.D. Augusto, M. Cristianini, *Braz. J. Food Technol.* **14**, 232–240 (2011)
16. F. Innings, C. Trägårdh, *Exp. Therm. Fluid Sci.* **32**, 345–354 (2007)
17. E. Dumay, D. Chevalier-Lucia, L. Picart-Palmade, A. Benzaria, A. Gràcia-Julià, C. Blayo, *Trends Food Sci. Technol.* **31**, 13–26 (2013)
18. M.A. Rao, in *Engineering Properties of Foods*, 3rd edn ed. By M.A. Rao, S.S.H. Rizvi, A.K. Datta, (CRC Press, Boca Raton: 2005)
19. V.M. Silva, A.C.K. Sato, G. Barbosa, G. Dacanal, H.J. Ciro-Velásquez, R.L. Cunha, *Int. J. Food Sci. Technol.* **45**, 2127–2133 (2010)
20. M.T.K. Kubo, P.E.D. Augusto, M. Cristianini, *Food Res. Int.* **51**(1), 170–179 (2013)
21. D.C.P. Campos, A.S. Santos, D.B. Wolkoff, V.M. Matta, L.M.C. Cabral, S. Couri, *Desalin.* **148**(6), 1–65 (2002)
22. P.M. Azoubel, D.C. Cipriani, A.A. El-Aouar, G.C. Antonio, F.E.X. Murr, *J. Food Eng.* **66**, 413–417 (2005)
23. C.C. Queiroz, F.F. Moreira, F.C. Lavinhas, M.L.M. Lopes, E. Fialho, V.L. Valente-Mesquita, *High Press. Res.* **30**(4), 507–513 (2010)
24. C.C. Queiroz, A.J.R. Silva, M.L.M. Lopes, E. Fialho, V.L. Valente-Mesquita, *Food Chem.* **125**, 128–132 (2011)
25. R.V. Tonon, D. Alexandre, M.D. Hubinger, R.L. Cunha, *J. Food Eng.* **92**, 425–431 (2009)
26. L.H. Fasolin, R.L. Cunha, *Cièn. Tecnol. Alim.* **32**(3), 558–567 (2012)
27. K.R.N. Moelants, R. Cardinaels, R.P. Jolie, T.A.J. Verrijssen, S. Van Buggenhout, L.M. Zumalacarregui, A.M. Van Loey, P. Moldenaers, M.E. Hendrickx, *Food Bioprocess Technol.* **6**(5), 1127–1143 (2013)
28. P.I. Figoni, C.F. Shoemaker, *J. Texture Stud.* **14**, 431–442 (1983)
29. B. Mert, *J. Food Eng.* **109**(3), 579–587 (2012)
30. D.B. Genovese, J.E. Lozano, M.A. Rao, *J. Food Sci.* **72**(2), R11–R20 (2007)
31. S. Croak, M. Corredig, *Food Hydrocol.* **20**, 961–965 (2006)
32. C. Servais, R. Jones, I. Roberts, *J. Food Eng.* **51**, 201–208 (2002)
33. P. Fischer, M. Pollard, P. Erni, I. Marti, S. Padar, C. R. Phys. **10**, 740–750 (2009)
34. D.B. Genovese, J.E. Lozano, *Food Hydrocoll.* **20**, 467–773 (2006)
35. P.E.D. Augusto, A. Ibarz, M. Cristianini, *J. Food Eng.* **111**, 474–477 (2012)

36. E.P.H.M. Schijvens, T. Van Vliet, C. Van Dijk, J. Texture Stud. **29**, 123–143 (1998)
37. S.C. Tsai, K. Zammouri, J. Rheol. **32**(7), 737–750 (1988)
38. A.J. Poslinski, M.E. Ryan, R.K. Gupta, S.G. Shehadri, F.J. Frechette, J. Rheol. **32**, 703–735 (1988)
39. E. Bayod, E.P. Willers, E. Tomberg, Food Sci. Technol. **41**(7), 1289–1300 (2008)
40. Z. Zhou, P.J. Scales, D.V. Boger, Chem. Eng. Sci. **56**, 2901–2920 (2001)
41. E. Cepeda, M.C. Villaran, A. Ibarz, J. Texture Stud. **30**, 481–491 (1999)
42. P.E.D. Augusto, V. Falguera, M. Cristianini, A. Ibarz, Int. J. Food Sci. Technol. **46**, 1086–1092 (2011)
43. J. Ahmed, H.S. Ramaswamy, K.C. Sashidhar, Food Sci. Technol. **40**, 225–231 (2007)
44. V. Falguera, A. Ibarz, Food Biophys. **5**, 114–119 (2010)
45. A.C.K. Sato, R.L. Cunha, J. Food Eng. **91**, 566–570 (2009)
46. P.E.D. Augusto, V. Falguera, M. Cristianini, A. Ibarz, Food Bioprocess Technol. **5**, 1715–1723 (2012)
47. C.W.I. Haminiuk, M.R. Sierakowski, G.M. Maciel, R.M.B. Vidal, I.G. Branco, M.L. Masson, Int. J. Food Eng. **2**(1), i–10 (2006)
48. A. Altan, S. Kus, A. Kaya, Food Sci. Technol. Int. **11**(2), 129–137 (2005)
49. S. Basu, U.S. Shivharey, G.S.V. Raghavan, Int. J. Food Eng. **3**(3), article 1 (2007)
50. R. Ravi, S. Bhattacharya, Int. J. Food Sci. Technol. **41**, 751–756 (2006)
51. D. Tavares, M.R. Alcantara, C.C. Tadini, J. Telis-Romero, Int. J. Food Prop. **10**(4), 829–839 (2007)
52. A.M. Ramos, A. Ibarz, J. Texture Stud. **29**, 313–324 (1998)